

Validation of the STORM response in IRI2000

E. A. Araujo-Pradere and T. J. Fuller-Rowell

NOAA Space Environment Center, Boulder, Colorado, USA

D. Bilitza

Raytheon ITSS, Goddard Space Flight Center, Greenbelt, Maryland, USA

Received 3 October 2002; revised 16 December 2002; accepted 22 January 2003; published 15 March 2003.

[1] The latest version of the International reference ionosphere, IRI2000 [Bilitza, 2001], contains a dependence on geomagnetic activity based on an empirical storm-time ionospheric correction model (STORM) [Araujo-Pradere *et al.*, 2002]. The new storm correction in IRI is driven by the previous time history (33 hours) of ap and is designed to scale the normal quiet-time F layer critical frequency (f_oF_2) to account for storm-time changes in the ionosphere. An extensive validation of IRI2000 has been performed during geomagnetic storm conditions to determine the validity of the new algorithms. The quality of the storm-time correction has been evaluated by comparing the model with the observed ionospheric response during all the geomagnetic storms with $ap > 150$ in 2000 and 2001, a total of 14 intervals. The model output was compared with the actual ionospheric response for all available ionosonde stations for each storm. The comparisons show that the model captures the decreases in electron density particularly well in summer and equinox conditions. To quantify the improvement in IRI2000, the root-mean-square error has been evaluated and compared with the previous version of IRI, which had no geomagnetic dependence. The results indicate that IRI2000 has almost a 30% improvement over IRI95 during the storm days and is able to capture more than 50% of the increase in variability, above quiet times, due to the storms. *INDEX TERMS:* 2447

Ionosphere: Modeling and forecasting; 2435 Ionosphere: Ionospheric disturbances; 2427 Ionosphere:

Ionosphere/atmosphere interactions (0335); *KEYWORDS:* ionosphere, empirical modeling, geomagnetic storm, IRI 2000, STORM model

Citation: Araujo-Pradere, E. A., T. J. Fuller-Rowell, and D. Bilitza, Validation of the STORM response in IRI2000, *J. Geophys. Res.*, 108(A3), 1120, doi:10.1029/2002JA009720, 2003.

1. Introduction

[2] Understanding the ionospheric response to the range of solar and geomagnetic variability is a challenge even with a complex physical model and is difficult to capture in a simple empirical algorithm. The response to a particular storm appears unique due to the complexity of the spatial and temporal variations in the driving processes from the magnetosphere and due to the many physical interactions coupling the thermosphere and ionosphere. However, data analysis and modeling have demonstrated that there are underlying trends in the ionospheric response that are consistent from one storm to the next, and it has been the goal of the recent empirical model development to capture these underlying trends. Although far from complete, this first step has characterized at least some of the common elements in the ionosphere response to storms in a relatively simple way.

[3] The ability to encapsulate complex physical processes in simple empirical representations is, in some way, a

measure of our understanding. Advances in our understanding of the ionospheric response to geomagnetic storms have evolved from analysis of data [Rodger *et al.*, 1989] and from numerical simulation using coupled thermosphere ionosphere models [e.g., Burns *et al.*, 1991; Fuller-Rowell *et al.*, 1994, 1996a]. The physical model simulations have illustrated how neutral composition changes respond and evolve during a storm as a function of latitude and season. It is this understanding that has guided the development of the simple empirical description, capturing at least part of the underlying trends in the ionospheric response, particularly those associated with neutral composition changes. The geomagnetic dependence recently included in IRI is based on the empirical storm-time ionospheric correction model STORM [Araujo-Pradere *et al.*, 2002; Araujo-Pradere and Fuller-Rowell, 2002; Fuller-Rowell *et al.*, 2001; Fuller-Rowell *et al.*, 1998]. The correction model has evolved from an analysis of an extensive database of ionosonde observations, guided by simulations using a coupled thermosphere-ionosphere model [Fuller-Rowell *et al.*, 1996b]. It is important to note that no part of the physical model is included in the empirical model, in order to maintain the tradition that IRI remains data driven.

[4] The international reference ionosphere is the most widely used empirical model and has been recommended as the international standard by the Committee on Space Research (COSPAR) and the International Union of Radio Science (URSI). These organizations formed a working group in the late 1960s to produce an empirical standard model of the ionosphere, based primarily on experimental evidence using all available data sources, and which has been updated periodically. One characteristic of the earlier versions was that they had no geomagnetic activity dependence; the recent release of IRI2000 [Bilitza, 2001] is the first version to include such dependence.

[5] Developing algorithms for updating of IRI parameters during storm-time conditions has been a high priority of the IRI team. First efforts were made by Kishcha [1995], which used 380 Northern Hemisphere substorm events to describe the changes in peak frequency (f_oF_2) and height (h_mF_2) as a function of the maximum AE index during the storm period [Bilitza, 1997]. The STORM model, the new IRI correction factor for geomagnetic perturbed conditions, used the long data record from ionosonde measurement to capture some of the common features of the ionospheric response to geomagnetic storms. Ionospheric data were sorted as a function of season and latitude and by the intensity of the storm. STORM uses a new geomagnetic index: the integral of ap over the previous 33 hours, with a weighting function deduced from regression analysis. In this work we refer to this index either as integrated ap or filtered ap .

[6] Araujo-Pradere [2002] performed a detailed study of the quality of the STORM model prediction for a particular site for the Bastille Day storm in July 2000. Araujo-Pradere and Fuller-Rowell [2001] considered the same storm but included a number of stations. Araujo-Pradere and Fuller-Rowell [2002] extended the validation to include all the storms in 2000. Now that the STORM model has been included into IRI2000, it is appropriate to perform a comprehensive evaluation of IRI. For this validation all storms in the years 2000 and 2001 where ap exceeded 150 were chosen. The output of IRI2000 is compared with all available F region critical frequencies (f_oF_2) from ionosonde stations around the world, for all the storms. The statistical results for IRI2000 are compared with IRI95 to evaluate the improvement, as a function of hemisphere and season.

2. IRI Overview

[7] The international reference ionosphere (IRI) was developed, and is updated periodically, by a joint working group of COSPAR and URSI. By charter, IRI is a data-driven model that attempts to represent the combined ionospheric data from ground and space measurements as accurately as possible. The group currently consists of experts representing different countries, measurement techniques, and modeling groups. More information about the working group members, goals, and progress (as well as information about software availability and links to IRI-related pages) can be found on the IRI home page at <http://nssdc.gsfc.nasa.gov/space/model/ionos/iri.html>. The basic model provides monthly averages of the electron and ion densities and temperatures. It captures the most important variation as a function of latitude, longitude, magnetic inclination (dip), local and universal

time, solar zenith angle, month, and solar activity. Details about the IRI model and the mathematical formalism can be found in the IRI-90 report [Bilitza, 1990]. The most recent version, IRI-2000, described by Bilitza [2001], includes the STORM empirical model as the correction for perturbed conditions and is available at ftp://nssdcftp.gsfc.nasa.gov/models/ionospheric/iri/iri2001/fortran_code/.

3. Storm Model Description

[8] A detailed description of the STORM model has been presented by Araujo-Pradere *et al.* [2002], so only a brief review will be presented here. The motivation behind the empirical model development is the data analysis study by Rodger *et al.* [1989] and the theoretical modeling work of Fuller-Rowell *et al.* [1996a, 1996b]. These investigations provided some insight and understandings into some of the expected dependencies in the ionospheric response to geomagnetic activity. The studies indicated that much of the consistent, repeatable characteristics of the storm-time ionosphere response could be attributed to long-lived thermospheric composition changes, which are driven by the integrated effect of Joule heating. It should be pointed out that the empirical algorithms that resulted from the storm analysis are based completely on data. The physical model simulations have only been used as a guide to the choice of sorting parameters. On the basis of this knowledge and guidance, a model taking into account the prior history of the geomagnetic index ap was designed [Araujo-Pradere *et al.*, 2002; Fuller-Rowell *et al.*, 2001].

[9] To develop the model, it was necessary to develop a new index based on a weighted integral of the previous 33 hours of the ap index. The optimum shape and length of the filter, shown in Figure 1, was obtained by the singular value decomposition method, minimizing the mean square difference between the filter input (ap index) and filter output (f_oF_2 ratios). Detman and Vassiliadis [1997] presented a good discussion of this technique. The dashed line in Figure 1 is the actual output of the numerical method, and the solid line is the fit used in the empirical model. The length of the filter, 33 hours, supports the well-established observation that the F region ionosphere takes 1–2 days to recover from a storm. The shape during the first 6 hours most likely reflects the complex dynamic and electrodynamic response of the upper atmosphere to the magnetospheric input. The longer-term filter response most likely reflects the development of storm-time composition changes.

[10] The previous data analysis and theory suggested a dominant seasonal-latitude dependence in the ionospheric response. With this in mind, data from 25 storms and 75 ionosonde stations were sorted as a function of geomagnetic latitude and season. The data were separated into a high (60° – 80°), low (0° – 20°), and two midlatitude bins (20° – 40° , 40° – 60°); and for solstices, equinox, and intermediate seasons as defined by Araujo-Pradere *et al.* [2002]. Within each latitude-seasonal bin, the nonlinear dependence of the filtered ap and the ionospheric response was determined. One example is shown in Figure 2 for midlatitude summer conditions. The figure shows the dependence of the ratio of the storm to quiet F region critical frequency (f_oF_2) as a function of the new storm index. The data show a clear dependence on the new index, with a progressively deeper

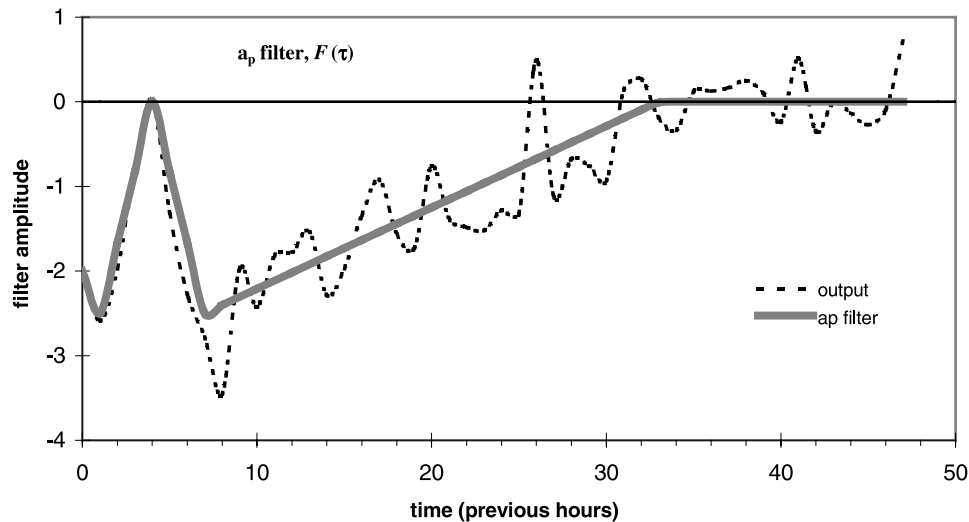


Figure 1. Optimum shape and length of the ap filter $F(\tau)$. The dashed line is the output of the method, and the solid line is the fit used as the ap filter in the model.

negative phase (ionospheric depletion) as the value of the filtered ap increases. Dependence up to second order (quadratic) is included in the model fit to the data. An estimate of the error on the fit to the data is also shown. The full range of seasonal and latitude conditions are given by Araujo-Pradere et al. [2002]. The model is triggered when the filtered ap exceeds 200 units, which is equivalent to an average ap of about 9 for the previous time history, or a Kp of 2^+ . This avoids making a correction of the IRI output for quiet conditions, for which the model is not designed.

[11] One interesting point is that the analysis by Rodger et al. [1989] showed a strong local time signature with a variation of about 40% in $N_m F_2$, which corresponds to a 20% signature in $f_o F_2$. We have been unable to show such a clear dependence in the present analysis, so we have not included the local time dependence at this time. The cause of the difference in the two analyses is unclear, but it may be due to the different indices used to sort the data.

[12] A real-time version of the STORM model has been implemented as an operational test product at the National Oceanic and Atmospheric Administration's Space Environment Center. The model is driven by the hourly values of the 3-hour running ap , as provided by the U.S. Air Force Hourly Magnetometer Analysis Reports. Hourly updates of the model predictions, in the middle and high latitude bands, can be found at <http://sec.noaa.gov/storm/>.

4. Validation

4.1. Data Sources and Storm Intervals

[13] To perform an authentic validation of the geomagnetic storm dependence in IRI2000, data from storms not included in the model development must be used. Fourteen storms have been selected in the years 2000 and 2001, covering a range of seasons and strengths of storms. Most are at moderately high solar activity, leaving a study of the model accuracy over a full solar cycle to a later work. Figure 3 shows the geomagnetic activity, as described by the ap index, for the 2000–2001 period. In this figure the date, maximum ap , and maximum Dst are shown for each

of the 14 storms that exceed an ap of 150. Note that 150 (shaded bar in Figure 3) is the threshold used by the NOAA for “strong” storms, classified as G3 on the NOAA Space Weather Scales (http://www.sec.noaa.gov/NOAA_scales/index.html). None of these events was included in the original database used to assemble the model, in accordance with the correct criteria for model validation [e.g., Pittock, 1978].

[14] During the validation period (2000–2001), nine storms occurred at the equinoxes, three occurred during solstices (May 2000, July 2000, and November 2001), and two occurred during the “intermediate” periods. This distribution, with more than 50% of the storms in the equinoxes, is consistent with previous finding of the equinox-preference for storms [Rishbeth and Mendillo, 2001, and references therein]. All of the storms were used in the validation.

[15] All available ground-based ionosonde data taken during the storms were used in the validation. Table 1 shows the ionosonde stations included in this study; for

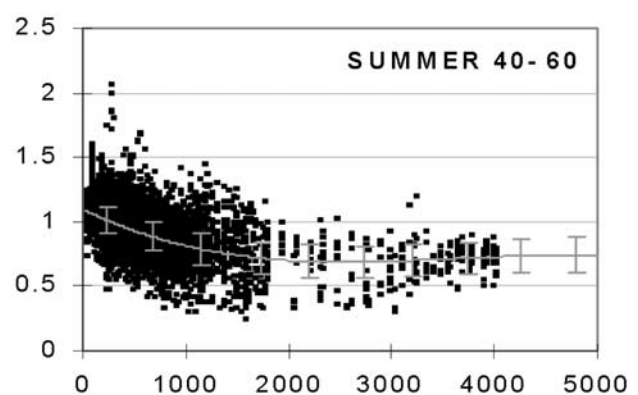


Figure 2. Nonlinear dependence of the ionospheric response (ratio $f_o F_2$) on the filtered ap at midlatitude (40–60 geomagnetic latitudes) summer conditions.

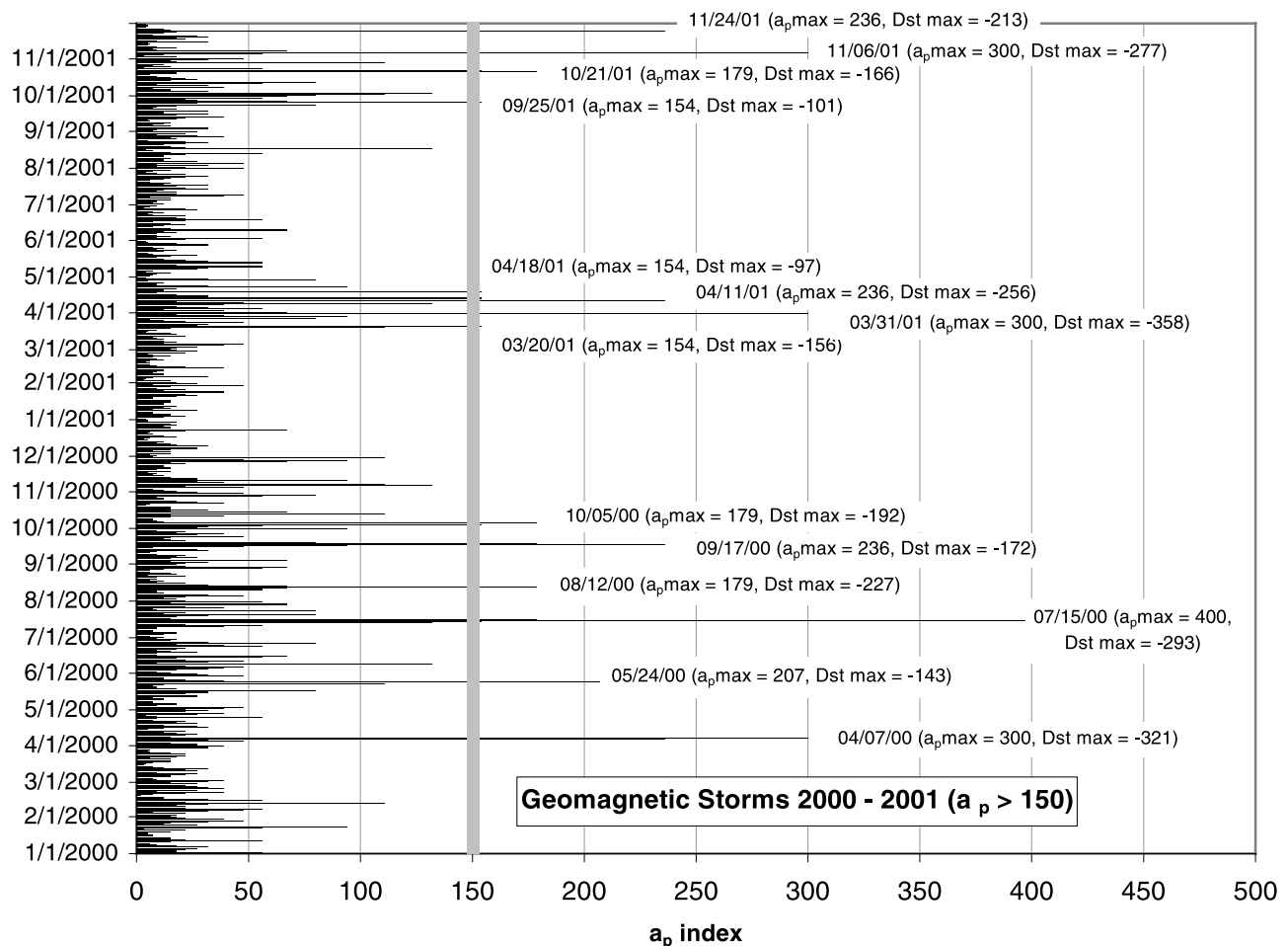


Figure 3. Geomagnetic activity for the period of interest, showing the 14 storms used in the validation.

each one the station code, the geographic coordinates, and geomagnetic latitude are given. The stations cover geomagnetic latitudes from 88.8 N to 51.4 S, with the best coverage at midlatitudes in the Northern Hemisphere.

[16] The only criterion in the selection of the stations was that data were available in the National Geophysical data Center (NGDC-NOAA) database and that there was reasonable continuity of the ionospheric data (f_oF_2) for the period of interest. All ionospheric data and geomagnetic indices were obtained from SPIDR, the Space Physics Interactive Data Resource (<http://spidr.ngdc.noaa.gov/spidr/>), an NGDC-NOAA Web site designed to allow solar terrestrial physics customers to access and manage historical space physics data.

[17] Ionosonde f_oF_2 measurements are fairly straightforward and can be considered as a direct measurement with little modeling involved. Traditionally, ionogram traces have been scaled manually and have the advantage that problems in the data can be spotted by an experienced operator. Most of the f_oF_2 data used for building the model were obtained manually.

[18] More recently, computer techniques have been employed for automatic scaling of ionogram profiles and for the extraction of h_mF_2 and f_oF_2 values. Although ideal and necessary for real-time applications, the quality of the parameters is sometimes questionable when no manual

intervention is applied. Most of the ionosonde data used for the current validation have relied on computer scaling. This undoubtedly has introduced errors, some of which are apparent in the figures. Lacking a good criteria to reject bad data points, all have been included; this must be kept in mind in the quantitative evaluation of STORM.

[19] For this work, f_oF_2 [MHz] hourly values for each site were used for a 5-day period of the storm (120 values) in order to see the full picture of the perturbed period including part of the quiet background. The focus of the quantitative analysis will be on the storm days, defined as the days when the Dst index was less than -100 nT at some time during the day [Araujo-Pradere et al., 2002]. These days tend to be when there was substantial deviation of the ionosphere from the monthly mean.

4.2. Statistical Analysis

[20] The response of the empirical storm-time correction model in IRI2000 has been tested for each 5-day interval of the storms in the 2000–2001 period. For the following statistical analysis, all the possible stations (i.e., stations with enough data) and storms were used in the study. In the interest of space, graphical examples will be more limited. As an example of the quality of IRI2000 in modeling storm conditions, Figure 4 compares the response of the ionosphere with the IRI prediction for 15 stations, for the storm

Table 1. Ionospheric Stations Used in the Validation Study

Number	Station	Code	Latitude	Longitude	Geomagnetic
					Latitude
1	Thule/Qanaq	THJ77	77.5	290.8	88.8
2	Narsarsuaq	NQJ61	61.2	314.6	70.9
3	King Salmon	KS759	58.4	203.6	63.5
4	Loparskaya	MM168	68.0	33.0	63.1
5	Salekhard	SD266	66.5	66.5	57.4
6	Leningrad	LD160	60.0	30.7	56.1
7	Juliusruh/Rugen	JR055	54.6	13.4	54.3
8	Millstome Hill	MHJ45	42.6	288.5	53.9
9	Podkamennaya	TZ362	61.6	90.0	50.8
10	Moscow	MO155	55.5	37.3	50.4
11	Chilton	RL052	51.6	358.7	49.9
12	Boulder	BC840	40.0	254.7	48.9
13	Petropavlosk	PK553	53.0	158.7	44.9
14	Novosibirsk	NS355	54.6	83.2	44.2
15	Tortosa	EB040	40.4	0.3	43.6
16	Rostov	RV149	47.2	39.7	42.4
17	Point Arguello	PA836	34.6	239.4	42.3
18	Dyess	DS932	32.4	260.3	42.0
19	Eglin AFB	EG931	30.4	273.3	41.1
20	Sofia	SQ143	42.7	23.4	41.0
21	Athens	AT138	38.0	23.6	36.4
22	San Vito	VT139	40.6	17.8	34.4
23	Tashkent	TQ241	41.3	69.6	32.3
24	Chongqing	09429	29.5	106.4	18.2
25	Darwin	DW41K	-12.4	130.9	-22.9
26	Learmonth	LM42B	-21.9	114.0	-33.0
27	Grahamstown	GR13L	-33.3	26.5	-33.9
28	Port Stanley	PSJ5J	-51.7	302.2	-40.6
29	Camden	CN53L	-34.0	150.7	-42.0
30	Hobart	HO54K	-42.9	147.2	-51.4

on 23–27 May 2000 (peak values of geomagnetic indices for this period were $ap = 207$ and $Dst = -143$). For this storm the maximum deviation from the monthly mean occurs on the second and third days of the period, which also correspond to our definition of so-called storm days, when Dst was less than -100 nT for at least part of the day. In the statistical comparison, we will focus particularly on these days. In contrast, Figure 5 illustrates the quality of the predictions as seen from a midlatitude station for all the storms included in the study. The station selected, Chilton (51.6°N , 358.7°E , geomagnetic latitude = 49.9°N), is well known for the high quality of the data, and it has one of the longest continuous records of ionospheric measurements.

[21] In Figures 4 and 5, for each storm and station, the time evolution of the hourly f_oF_2 [MHz] is displayed, together with the prediction from both versions of the IRI empirical model. The solid line represents the observed F region critical frequency (f_oF_2), while the shaded dashed line and the shaded solid line are the IRI95 and the IRI2000 outputs, respectively. At the bottom of each panel appear the values of the daily-normalized root-mean-square error ($\text{RMSE} = ((\sum(\text{model} - \text{data})^2)/24)^{0.5}$) for both versions of IRI. The daily value of the RMSE is the metric used to quantify the accuracy of the predictions in this study; the circles depict the value for IRI2000 and the crosses are for IRI95, over the previous 24-hour periods. The x-axis corresponds to time, from 0000 UT on the first day of the period (23 May) up to the 120th hour. The y-axis is the value of f_oF_2 for both the data and the models output. The y-axis also quantifies the RMSE.

[22] As mentioned before, in Figures 4 and 5, there are occasional data values that may be questionable, such as

what appear to be data spikes. In the following statistic analysis all of the data are used in the calculation of the RMSE, including the questionable points, to avoid the inappropriate removal of real data points that do not fit the model.

[23] Figures 4 and 5 visually demonstrate the improved ability of IRI2000, compared with IRI95. In most cases, IRI2000 is able to capture the direction of the observed ionospheric changes. For nonstorm days there is not a considerable difference between the prediction of IRI95 and IRI2000 (note that the storm days are different for each storm period), and usually they both follow the observations. During summer, the data tends toward a negative phase, which is generally captured well by IRI2000; IRI95 of course does not react to the perturbed conditions. For winter conditions the data are more variable, do not exhibit such a clear trend, and are more difficult to predict. The lack of a clear direction of the ionospheric response in winter makes model predictions challenging, but at least IRI2000 does not over-predict the response. For equinox conditions, IRI2000 output shows a good agreement with the observations, capturing the predominant negative phase in both direction and magnitude.

[24] The quality of the IRI2000 prediction during “intermediate” seasons (between the equinox and solstices) is also depicted in Figure 5. From this set of storms, only 20–24 October 2001 and 5–9 November 2001 fulfill the intermediate definition, and both show a noticeable improvement in IRI2000. Note also that the response for the 23–27 November 2001 storm, just 2 weeks later, has a very different character. In the empirical storm model classification [Araujo-Pradere and Fuller-Rowell, 2002], late November corresponds to winter, whereas early November is classified as intermediate. The observations indicate that for this station, these two storms in the same calendar month have a different response. The earlier storm shows a negative phase, and the later storm indicates little change. IRI2000 follows both reasonably well; the predictions of IRI95 and IRI2000 are almost identical for the storm in late November.

[25] The sample of data in Figures 4 and 5 provides a good visual indication that IRI2000 is significantly improved over IRI95. The following figures and statistics include the results from all the storms and for all the stations. Figure 6 shows, for each storm, the average RMSE for all stations on the storm days. In this figure, solid diamonds represent the RMSE for IRI95, and the solid circles correspond to IRI2000. In order to clearly show the correspondence of these values for each storm, a solid line connects both symbols. Next to each circle is the date of the storm.

[26] A general picture of the quality of IRI2000 prediction is obtained from Figure 6; IRI2000 shows a consistent improvement over IRI95 for all the storms in the validation period. The magnitude of the improvement depends primarily of the season, being the best in northern summer and equinoxes and the smallest in winter. The asymmetry in the distributions of stations in the Northern and Southern Hemispheres is partly influencing the results.

[27] Figure 7 illustrates a different approach to quantifying the overall accuracy. The RMSE for each station is shown, averaged over all the storm days, from the northernmost station (Thule/Qanaq) to the most southern (Hobart). In this

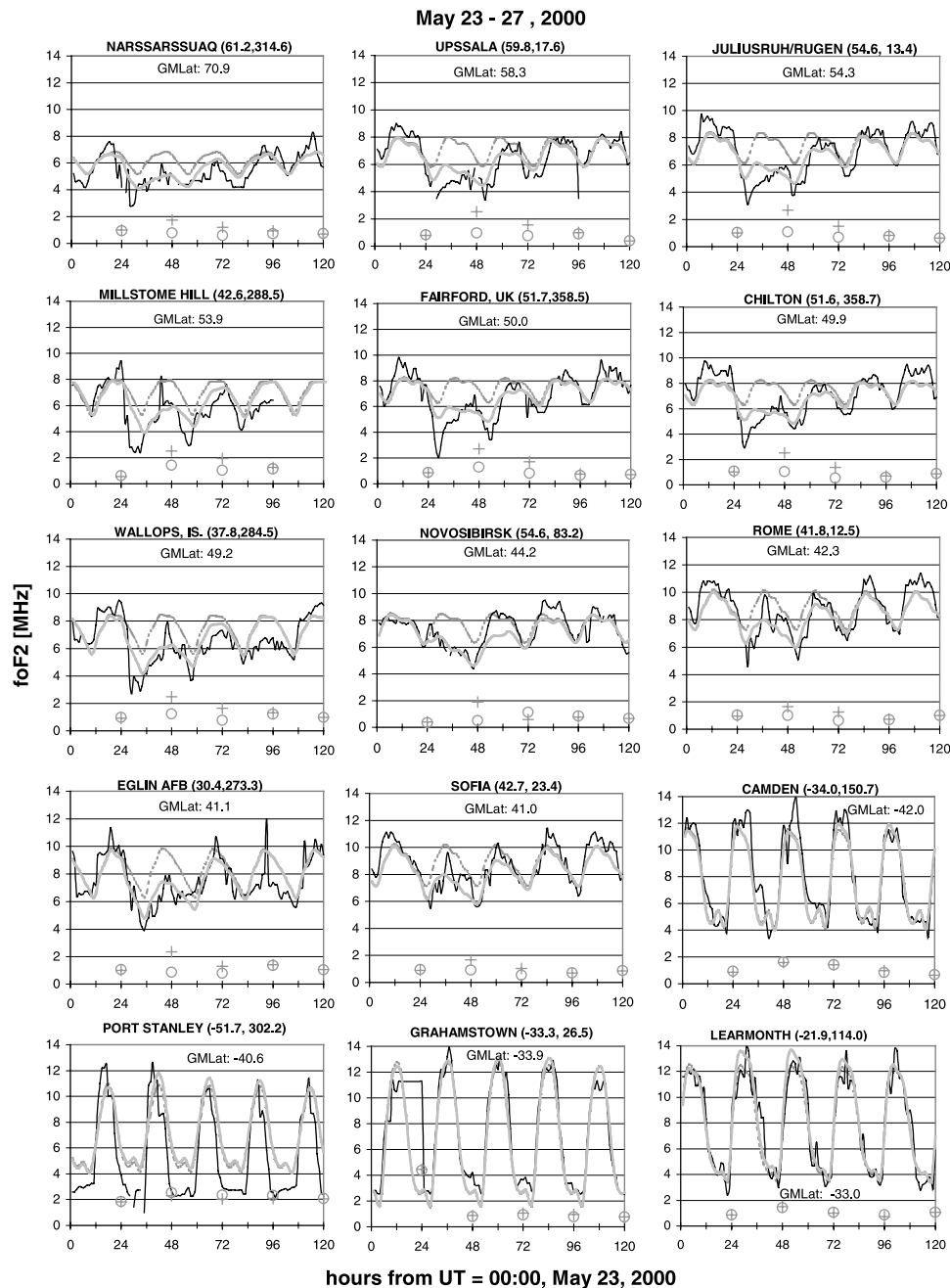


Figure 4. Data and output of the IRI95 and IRI2000 models at 15 different locations for the May 2000 storm. The dashed shaded line shows IRI95, the solid line is the observation, and the solid shaded line shows IRI2000. Note that for Southern Hemisphere stations (winter), the output of IRI95 and IRI2000 are almost coincident, so that the dashed shaded line is sometimes hidden behind the solid shaded line.

figure the open bars represent IRI95 and the shaded bars are IRI2000. It is important to mention that for some stations data are not available for all storms. The average RMSE for each station shown in Figure 7 depicts a general improvement for most of the stations, while for some (e.g., Athens, Dyess, and College) it is just marginal and within the day-to-day variability of the data, which will be discussed later.

[28] The best results correspond to some of the Northern Hemisphere midlatitude stations, where there are improvements up to a 50% for some sites (e.g., Moscow, Chilton,

and Wallops Island). Surprisingly, the quality of the predictions at high latitudes is reasonable, showing some improvement of IRI2000 over IRI95.

[29] Figures 6 and 7 offer an encouraging picture of the improvement reached by IRI2000. To finally quantify the accuracy, Table 2 shows the results of the statistical analysis for all the perturbations in the 2000–2001 period. For each of the 14 storms, the RMSE is shown for every day of the 5-day intervals for both IRI95 and IRI2000, averaged over all available stations in the Northern and Southern Hemispheres separately.

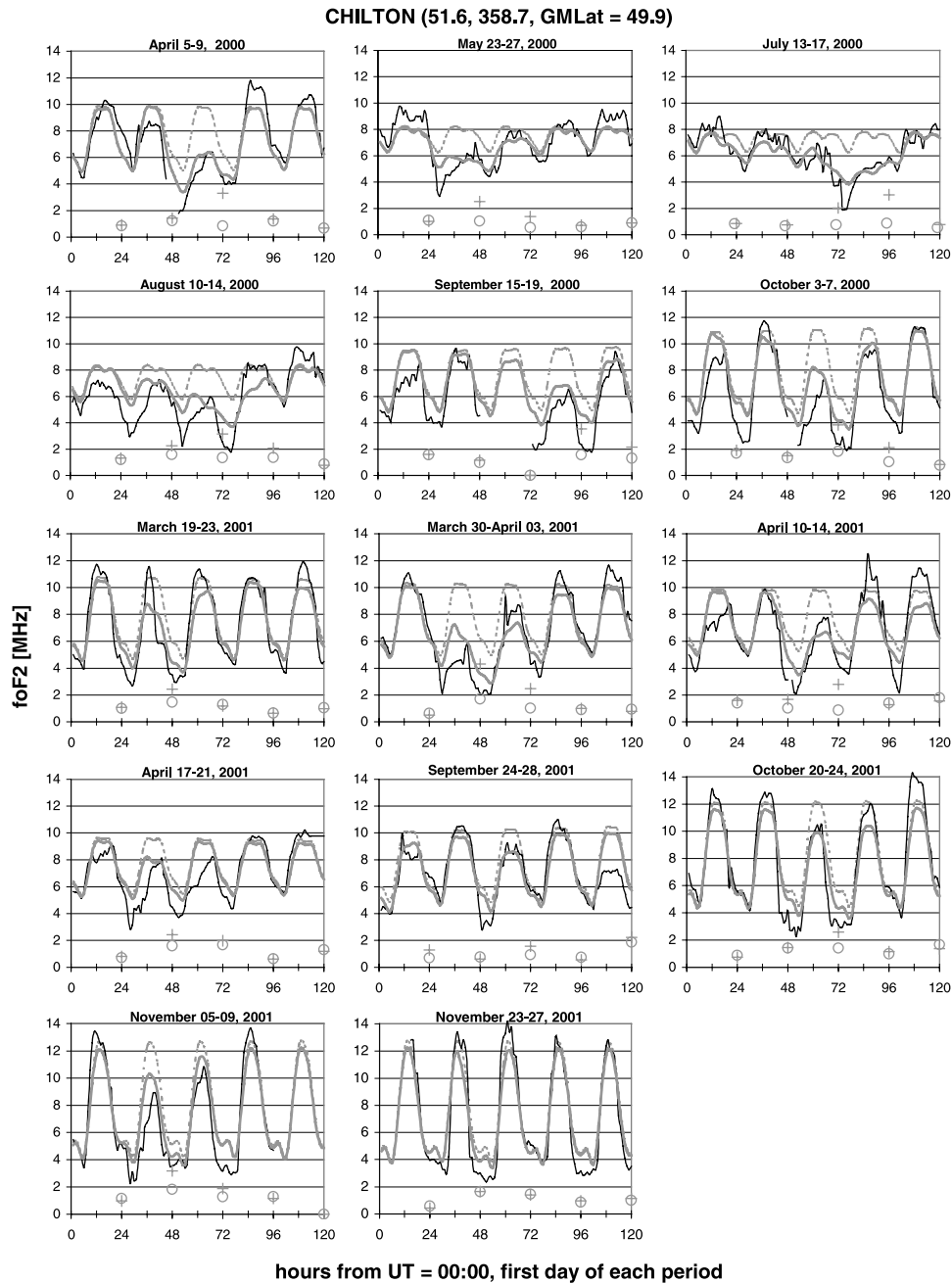


Figure 5. Data and output of the IRI95 and IRI2000 models at Chilton for all the storms in the 2000–2001 period. The dashed shaded line shows IRI95, the solid line is the observation, and the solid shaded line shows IRI2000. Note that for the winter storm (23–27 November), the outputs of IRI95 and IRI2000 are almost coincident, so that the dashed shaded line is sometimes hidden behind the solid shaded line.

[30] In this table the storm days and the corresponding averages are shown in bold. The “averages” columns show the average RMSE for all 5 days and for the storm day or days. The improvement of IRI2000 over IRI95 on the storm days is also shown as a percentage (% imp), and is given by the expression

$$\% \text{ imp} = ((\text{RMSE}(\text{IRI95}) - \text{RMSE}(\text{IRI2000})) / \text{RMSE}(\text{IRI95})) \times 100.$$

Eight of the cases lie within $\pm 6\%$, indicating no significant change in the accuracy of the prediction. These cases tend to cluster around the winter hemisphere, a known weak area for the model. All the other 20 cases show significant improvement. Considering all the storm days, the STORM model improves the prediction of IRI by 34% in the Northern Hemisphere and a 20% in the Southern Hemisphere, an overall “global” improvement in performance of 28%. The result for the particular case of May 2000, presented in Figure 3, is one of the better cases for the

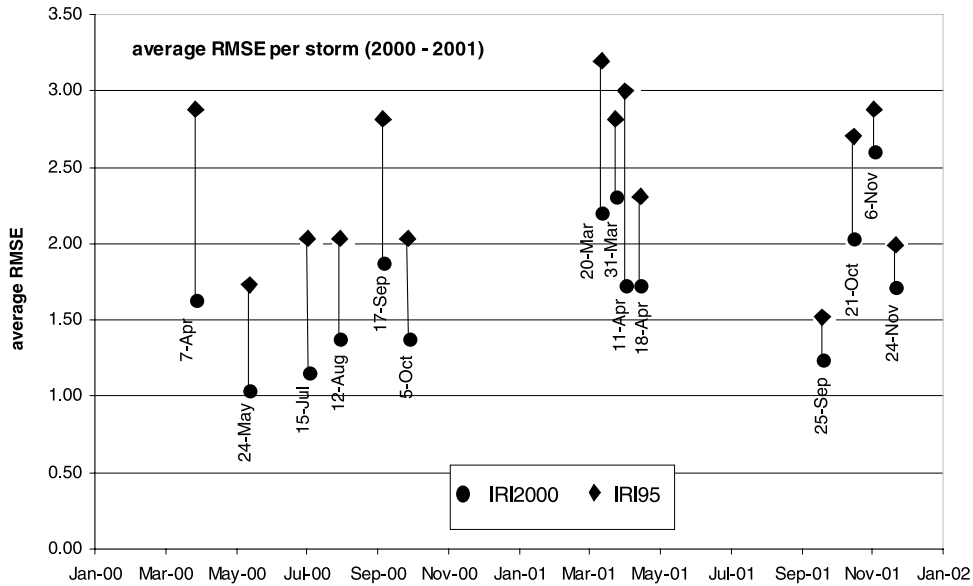


Figure 6. Average storm day root-mean-square error, including all stations, for each storm.

summer hemisphere, with IRI2000 showing a 51% improvement over IRI95 for storm days.

[31] Since quiet days also have geophysical variability, it is useful to estimate how much of the increase in standard deviation during the storm days is captured by the model. During the quiet days preceding the storms, or nonstorm days, the variability of the data around the monthly mean (standard deviation of the data) is about 13%, very close to previous results [Araujo-Pradere and Fuller-Rowell, 2000],

and during the storm days the standard deviation increases to about 27%. The STORM model reduces this standard deviation to 19%, which implies that the STORM model is capturing more than half of the storm-induced variability (for a more detailed discussion concerning the error bars of the STORM model, see Araujo-Pradere and Fuller-Rowell [2002]).

[32] From the results described in the previous paragraph, changes within $\pm 10\%$ can generally be considered as being

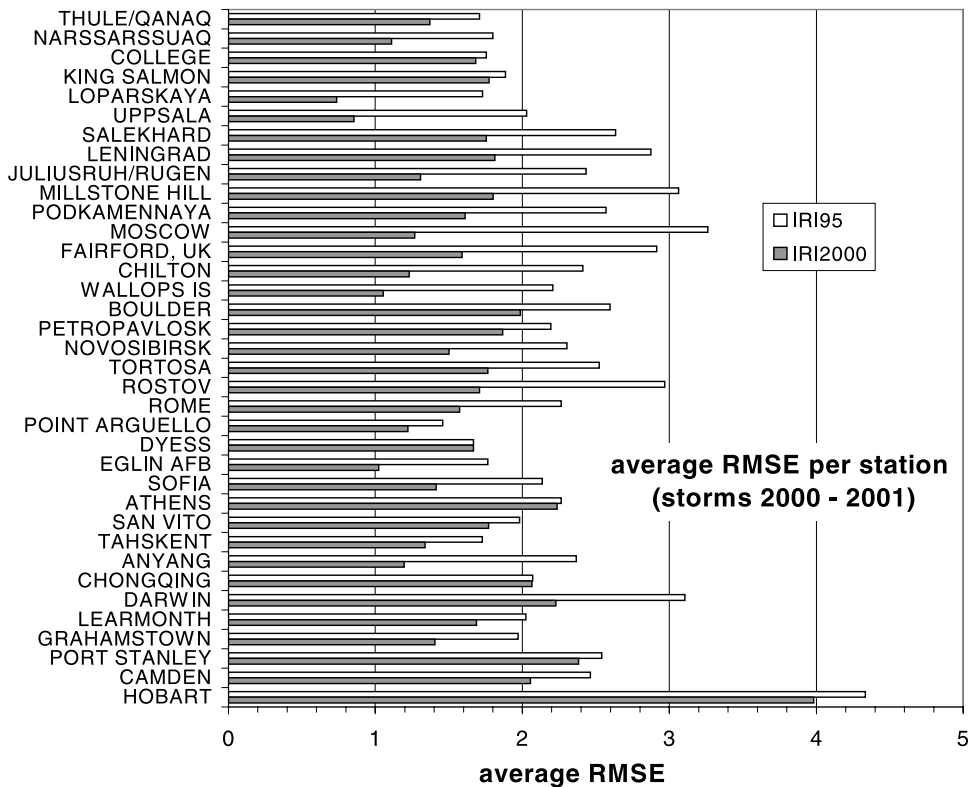


Figure 7. Average storm day root-mean-square error, including all storms, for each station.

Table 2. A Comprehensive Validation of the STORM Response in IRI2000^a

		Northern Hemisphere							Southern Hemisphere								
		Days					Averages		%	Days					Averages		%
		1	2	3	4	5	Storm	Storm Day	Imp	1	2	3	4	5	Storm	Storm Day	Imp
7 April	IRI95	1.22	1.26	2.88	1.30	0.91	1.51	2.88	49	1.94	1.82	3.03	1.59	1.70	2.02	3.03	31
2000	IRI00	1.19	1.18	1.45	1.33	0.91	1.21	1.45		1.94	1.88	2.10	1.72	1.70	1.87	2.10	
24 May	IRI95	0.86	2.25	1.37	0.95	0.79	1.24	1.81	51	2.00	1.56	1.38	1.18	1.13	1.45	1.47	-3
2000	IRI00	0.89	1.01	0.76	0.87	0.79	0.86	0.88		2.01	1.60	1.44	1.20	1.14	1.48	1.52	
15 July	IRI95	1.03	0.96	1.70	2.75	1.08	1.51	2.23	49	1.17	1.07	1.19	1.33	1.27	1.20	1.26	-6
2000	IRI00	0.90	0.85	1.05	1.21	0.82	0.97	1.13		1.20	1.19	1.16	1.51	1.27	1.26	1.33	
12 Aug.	IRI95	1.24	1.94	2.94	1.99	1.14	1.85	2.29	40	1.16	1.28	1.56	1.17	1.10	1.25	1.34	-5
2000	IRI00	1.17	1.47	1.50	1.18	1.13	1.29	1.38		1.15	1.28	1.55	1.36	1.08	1.28	1.40	
17 Sept.	IRI95	1.43	1.50	2.05	3.36	2.28	2.12	2.70	38	2.01	1.80	2.57	3.59	2.06	2.41	3.08	22
2000	IRI00	1.37	1.31	1.63	1.74	1.54	1.52	1.69		1.74	1.67	2.24	2.58	1.74	2.00	2.41	
5 Oct.	IRI95	1.80	1.74	2.75	1.64	0.92	1.77	2.04	32	0.78	1.62	3.68	1.55	1.00	1.72	2.28	32
2000	IRI00	1.63	1.46	1.63	1.06	0.87	1.33	1.38		0.72	1.33	2.26	1.09	0.99	1.28	1.56	
20 March	IRI95	1.14	2.83	1.53	0.97	1.46	1.58	2.83	37	1.83	4.23	2.46	1.06	1.18	2.15	4.23	19
2001	IRI00	1.06	1.80	1.38	0.88	1.23	1.27	1.80		1.90	3.44	1.85	1.01	1.05	1.85	3.44	
31 March	IRI95	0.88	3.28	2.04	1.30	1.26	1.75	2.66	34	2.01	3.10	3.79	1.49	1.34	2.35	3.45	-3
2001	IRI00	0.98	1.85	1.67	1.22	1.37	1.42	1.76		2.17	3.55	3.52	1.61	1.47	2.47	3.54	
11 April	IRI95	1.63	1.49	2.63	1.62	1.88	1.85	2.63	48	1.21	1.66	3.94	1.56	2.99	2.27	3.94	31
2001	IRI00	1.54	1.31	1.36	1.35	1.59	1.43	1.36		1.21	1.55	2.72	1.46	2.51	1.89	2.72	
18 April	IRI95	0.98	2.43	1.60	0.86	0.59	1.29	2.43	31	1.21	2.10	1.82	1.45	1.28	1.57	2.10	6
2001	IRI00	0.87	1.66	1.36	0.79	0.58	1.05	1.66		1.24	1.97	1.85	1.42	1.25	1.54	1.97	
25 Sept.	IRI95	1.78	0.98	1.70	1.38	1.37	1.44	1.70	31	1.70	1.08	1.01	1.12	1.65	1.31	1.01	-5
2001	IRI00	1.34	0.94	1.17	1.29	1.17	1.18	1.17		1.25	1.14	1.07	1.21	1.71	1.27	1.07	
21 Oct.	IRI95	0.86	1.55	2.54	1.76	1.19	1.58	2.54	18	0.83	1.09	3.16	2.10	1.13	1.66	3.16	47
2001	IRI00	1.07	1.56	2.10	1.44	1.37	1.51	2.10		0.93	1.33	1.67	1.92	1.32	1.43	1.67	
6 Nov.	IRI95	1.22	2.69	1.54	1.53	1.05	1.60	2.69	5	0.96	3.55	1.83	1.61	1.00	1.79	3.55	23
2001	IRI00	1.36	2.54	1.48	1.52	1.05	1.59	2.54		1.08	2.72	1.88	1.60	1.12	1.68	2.72	
24 Nov.	IRI95	1.02	1.72	1.08	1.11	1.32	1.25	1.72	1	1.05	2.59	1.52	1.11	0.99	1.46	2.59	33
2001	IRI00	1.06	1.71	1.17	1.01	1.17	1.22	1.71		0.94	1.73	1.15	1.08	1.08	1.20	1.73	

^aThe root-mean-square error, in megahertz, for IRI2000 (in the table identify as IRI00) and IRI95 is shown for each day of the 5-day storm periods, averaged over Northern and Southern Hemisphere separately. Actual storm days are in bold.

essentially no change, as this probably reflects the day-to-day variability in the data. Therefore, from the 28 cases discussed, in eight cases (29%) IRI2000 was similar to the prediction of IRI95, while in all of the other 20 cases (71%) IRI2000 offers a noticeable improvement over IRI95.

5. Discussion

[33] The prospects for further development of STORM will be limited by our understanding of the physics of the response. The present algorithm has been based largely on three basic ideas: first, that the integrated effect of Joule heating drives upwelling and composition changes, leading to depletions in the *F* region ionosphere; second, that the seasonal circulation transports composition changes to mid-latitudes, particularly during the summer seasons; and third, that composition bulges recover slowly in the aftermath of the storms.

[34] Known problems in winter for STORM arise from two sources. The first involves the boundary between increases and decreases in molecular neutral species that exists at midlatitudes. The location of this boundary is difficult to predict with accuracy, since it depends on the magnitude of the storm forcing. In particular, it depends on the location and strength of the Joule heating upwelling and the boundary between the quiet background and the storm circulation, none of which is well known for a given storm. An uncertainty of $\pm 10^\circ$ in this boundary is quite likely, making predictions at winter midlatitude particularly challenging.

[35] A second fact influences the winter hemisphere. In the summer hemisphere, even during quiet times, molecular neutral species are more prevalent at *F* region altitudes due to the global circulation. The ionosphere is therefore more composition controlled and so is impacted less by changes in neutral winds. In contrast, in winter, wind changes have a bigger impact at the *F* region plasma densities, leading to a general increase in variability. During a storm, when neutral winds are large, dynamic, and very difficult to predict, the winter hemisphere is more susceptible to these dynamic wind changes and contributes greatly to the difficulties in predicting the response.

[36] In the early phases of a storm, magnetosphere electron fields penetrate to midlatitudes and profoundly affect plasma structure through transport and stripping away the plasmopause [Foster *et al.*, 2002]. This is certainly an area where improvements could be made to STORM, but will require improved understanding of the physics.

[37] Another area that requires improvement is the low latitudes. Again, our understanding of the physics is rudimentary, so the prospects of capturing the storm response in an empirical model are unlikely. New coupled models of the thermosphere-ionosphere-plasmasphere are beginning to probe the equatorial region and hopefully hold promise for the future.

6. Conclusion

[38] An extensive validation of IRI2000, which now includes a dependence on geomagnetic activity, has been

performed covering all the geomagnetic storms in 2000–2001. Ionospheric data at an average of 15 sites for each storm were compared with the prediction from IRI2000 and with the previous version, IRI95, which had no geomagnetic dependence. The accuracy of the model has been quantified by evaluating the RMSE between the model and observations and comparing the prediction with the previous version of IRI. For the storms considered, the results showed that IRI2000 is 34% improved over IRI95 in the Northern Hemisphere, 20% in the Southern Hemisphere, and up to 50% for the Northern Hemisphere in summer. IRI2000 is also able to capture more than 50% of the increase in variability due to the storms.

[39] **Acknowledgments.** This work was partially supported by NSF grant ATM-9713440.

[40] Arthur Richmond thanks Ludger Scherliess and Philip Wilkinson for their assistance in evaluating this paper.

References

- Araujo-Pradere, E. A., Quality of the STORM model prediction for a mid-latitude station, *Geofis. Int.*, *41*(2), 195–201, 2002.
- Araujo-Pradere, E. A., and T. J. Fuller-Rowell, A model of a perturbed ionosphere using the auroral power as the input, *Geofis. Int.*, *39*(1), 29–36, 2000.
- Araujo-Pradere, E. A., and T. J. Fuller-Rowell, Evaluation of the STORM time ionospheric empirical model for the Bastille Day event, *Sol. Phys.*, *204*(1), 315–322, 2001.
- Araujo-Pradere, E. A., and T. J. Fuller-Rowell, STORM: An empirical storm-time ionospheric correction model, 2, Validation, *Radio Sci.*, *37*(5), 1071, doi:10.1029/2002RS002620, 2002.
- Araujo-Pradere, E. A., T. J. Fuller-Rowell, and M. V. Codrescu, STORM: An empirical storm-time ionospheric correction model, 1, Model description, *Radio Sci.*, *37*(5), 1070, doi:10.1029/2001RS002467, 2002.
- Bilitza, D., International reference ionosphere 1990, World Data Cent. for Rockets and Satellites, Greenbelt, Md., 1990.
- Bilitza, D., International reference ionosphere-Status 1995/96, *Adv. Space Res.*, *20*(9), 1751–1754, 1997.
- Bilitza, D., International reference ionosphere 2000, *Radio Sci.*, *36*(2), 261–275, 2001.
- Burns, A. G., T. L. Killeen, and R. G. Roble, A theoretical study of thermospheric composition perturbations during an impulsive geomagnetic storm, *J. Geophys. Res.*, *96*, 14,153–14,167, 1991.
- Detman, T. R., and D. Vassiliadis, Review of techniques for magnetic storm forecasting, in *Magnetic Storms, Geophys. Monogr. Ser.*, vol. 98, edited by B. Tsurutani et al., pp. 253–266, AGU, Washington, D. C., 1997.
- Foster, J. C., P. J. Erickson, A. J. Coster, J. Goldstein, and F. J. Rich, Ionospheric signatures of plasmaspheric tails, *Geophys. Res. Lett.*, *29*(13), 1623, doi:10.1029/2002GL015067, 2002.
- Fuller-Rowell, T. J., M. V. Codrescu, R. J. Moffet, and S. Quegan, Response of the thermosphere and ionosphere to geomagnetic storms, *J. Geophys. Res.*, *99*, 3893–3914, 1994.
- Fuller-Rowell, T. J., M. V. Codrescu, R. J. Moffet, and S. Quegan, On the seasonal response of the thermosphere and ionosphere to geomagnetic storms, *J. Geophys. Res.*, *101*(A2), 2343–2353, 1996a.
- Fuller-Rowell, T. J., D. Rees, S. Quegan, R. J. Moffett, M. V. Codrescu, and G. H. Millward, A coupled thermosphere-ionosphere model (CTIM), in *STEP: Handbook of Ionospheric Models*, edited by R. W. Schunk, pp. 217–238, Utah State Univ., Logan, Utah, 1996b.
- Fuller-Rowell, T. J., M. V. Codrescu, E. A. Araujo-Pradere, and I. Kutiev, Progress in developing a storm-time ionospheric correction model, *Adv. Space Res.*, *22*(6), 821–827, 1998.
- Fuller-Rowell, T. J., M. V. Codrescu, and E. A. Araujo-Pradere, Capturing the storm-time *F* region ionospheric response in an empirical model, in *Space Weather, Geophys. Monogr. Ser.*, vol. 125, edited by P. Song, J. Singer, and G. L. Siscoe, pp. 393–401, AGU, Washington, D. C., 2001.
- Kishcha, P. V., Indices and updating procedures for modeling of ionospheric disturbances, *Adv. Space Res.*, *22*(1), 55–64, 1995.
- Pittock, A. B., A critical look at long-term Sun-weather relationships, *Rev. Geophys.*, *16*(3), 400–420, 1978.
- Rishbeth, H., and M. Mendillo, Patterns of *F*₂-layer variability, *J. Atmos. Sol. Terr. Phys.*, *63*, 1661–1680, 2001.
- Rodger, A. S., G. L. Wrenn, and H. Rishbeth, Geomagnetic storms in the Antarctic *F* region, II, Physical interpretation, *J. Atmos. Terr. Phys.*, *51*, 851–866, 1989.

E. A. Araujo-Pradere and T. J. Fuller-Rowell, NOAA Space Environment Center, 325 Broadway, Boulder, CO 80305, USA. (eduardo.araujo@noaa.gov)

D. Bilitza, Raytheon ITSS, Goddard Space Flight Center, Code 632, Greenbelt, MD 20771, USA.